Saudi Journal of Biological Sciences 28 (2021) 6592–6605

Contents lists available at ScienceDirect

Saudi Journal of Biological Sciences

journal homepage: www.sciencedirect.com

Original article

Biochemical and *in silico* study of leaf and bark extracts from *Aphanamixis polystachya* against common pathogenic bacteria

Gobindo Kumar Paul [1], Shafi Mahmud [1], Md. Mehedi Hasan, Shahriar Zaman, Md. Salah Uddin *, Md. Abu Saleh *

Microbiology Laboratory, Department of Genetic Engineering and Biotechnology, University of Rajshahi, Rajshahi 6205, Bangladesh

ARTICLE INFO

Article history:
Received 5 May 2021
Revised 29 June 2021
Accepted 8 July 2021
Available online 16 July 2021

Keywords:
Aphanamixis polystachya extract
Antibiotic resistance
Antimicrobial activity
Antioxidant activity
Cytotoxicity
Molecular docking

ABSTRACT

Aphanamixis polystachya may be a natural, renewable resource against antibiotic-resistant bacterial infections. The antibacterial activity of *A. polystachya* leaf and bark extracts was investigated against three antibiotic-resistant bacterial species and one fungus. Methanolic leaf extract showed only limited antibacterial activity but both methanolic and aqueous bark extract showed high antimicrobial activity. In an antioxidant activity test, leaf and bark extracts exhibited 50% free radical scavenging at a concentration of 107.14 ± 3.14 μg/mL and 97.13 ± 3.05 μg/mL, respectively, indicating that bark extracts offer more antioxidative activity than leaf extracts. Bark extracts also showed lower toxicity than leaf extracts. This suggests that bark extracts may offer greater development potential than leaf extracts. The molecular dynamics were also investigated through the simulated exploration of multiple potential interactions to understand the interaction dynamics (root-mean-square deviation, solvent-accessible surface area, radius of gyration, and the hydrogen bonding of chosen compounds to protein targets) and possible mechanisms of inhibition. This molecular modeling of compounds derived from *A. polystachya* revealed that inhibition may occur by binding to the active sites of the target proteins of the tested bacterial strains. *A. polystachya* bark extract may be used as a natural source of drugs to control antibiotic-resistant bacteria.

1. Introduction

The pathogenic microbial species that alter normal body function are structurally or physiologically complicated and cause many infectious diseases due to their antibiotic (Bhavsar et al., 2007) and drug resistance (Amenu, 2014). Pathogenic *Streptococcus* sp. are involved in skin and respiratory infections (Brouwer et al., 2016), while *E. coli* and *Pseudomonas* sp. cause urological and gastrointestinal diseases (Zalewska-Piątek and Piątek, 2020). The extensive use of antibiotics is the main factor in the development of infectious microbes' resistance to treatment (Pendleton et al., 2013). Some antimicrobial agents increase these microbes' resistance against such commercially available antibiotics as gentamicin, penicillin, ciprofloxacin, erythromycin, tobramycin, clindamycin, chloramphenicol, and vancomycin (Franklin, 2003). The World Health Organization (WHO) reported that nearly 50,000 people die every day due to antibiotic-resistant infections (Khademi et al., 2012), and 65% to 80% of the world also depends on traditional medicine (Kaur and Arora, 2009). Local plants may provide solutions for the control of infectious diseases. There are an estimated 250,000 to 500,000 plant species in the world and only a few have been studied to determine the uses of their phytochemicals (Mahesh and Satish, 2008). Plant extracts are of great interest to researchers seeking new drugs to treat antibiotic-resistant microorganisms (Rayne and Mazza, 2007; Suffredini et al., 2004).

Alkaloids, phenols, flavonoids, and tannins are essential secondary metabolites that have been found in plants and showed antimicrobial properties (Djeussi et al., 2013; Duraipandiyan et al., 2006). These plants have increased potential for the pharmaceutical and medical industries due to their bioactive compounds

* Corresponding author at: Department of Genetic Engineering and Biotechnology University of Rajshahi, Rajshahi 6205, Bangladesh.
E-mail addresses: salim.geb@ru.ac.bd (M.S. Uddin), saleh@ru.ac.bd (M.A. Saleh).

[1] Co-First Author.

Peer review under responsibility of King Saud University.

Production and hosting by Elsevier

https://doi.org/10.1016/j.sjbs.2021.07.032
1319-562X/

(Joana Gil-Chávez et al., 2013). Several studies showed that plant species such as *Moringa oleifera* (Zaffer et al., 2014), *Syzygium cumini* (Prasad and Swamy, 2013), *Aphanamixis polystachya* (Rahman et al., 2017), *Azadirachta indica* (Francine et al., 2015), and *Aegle marmelos* (Poonkothai and Saravanan, 2008), among others, have antibacterial activity against pathogenic bacterial species. Many plants with antioxidant properties have beneficial health effects as well (Gayathri Devi et al., 2013; Subba and Basnet, 2014). Free radicals in the body lead to oxidative stress and are responsible for mechanisms of cancer, atherosclerosis, diabetes, and neurodegenerative and inflammatory diseases (Liguori et al., 2018; Lushchak, 2014; R. et al., 2014). Antioxidants can delay oxidation by scavenging free radicals and reducing oxidative stress (Carocho and Ferreira, 2013; Tiwari, 2004).

Despite their therapeutic potential, many plants have toxic effects on normal body cell functions (Baravalia et al., 2012). The present study aims to determine the pharmacological and toxicological action of *A. polystachya* leaves and bark. A brine shrimp lethality assay is an effective and advisable test for the preliminary assessment of toxicity (Manilal et al., 2009; Waghulde et al., 2019) and this method can be performed with plant extracts to facilitate the isolation of biologically active compounds (Pisutthanan et al., 2004).

The present study aims to investigate the antimicrobial, antioxidant, and cytotoxic activity of *A. polystachya* leaf and bark extracts under laboratory conditions. In addition, the proposed drugs were investigated in a simulated human body environment (Poojary, 2020). This method is both cost- and time-effective for understanding the correlation between proteins and ligands (Mahmud et al., 2021a, 2020b). The results of this investigation revealed high antibacterial and antioxidant activity with reduced toxicity in *A. polystachya* bark. *In silico* analysis was used to identify likely compounds from *A. polystachya* bark with the potential to bind to active sites in antibiotic-resistant bacteria and inhibit their activity. Molecular dynamics tests were performed to predict the formation of convenient ligand-receptor complexes with optimized conformations.

2. Materials and methods

2.1. Plant sample collection and authentication

A. polystachya leaves and bark samples were collected from different locations on the University of Rajshahi (Rajshahi, Bangladesh) campus and disease-free samples were placed in a sterile zip bag for transport to the Microbiology Laboratory in the Department of Genetic Engineering and Biotechnology at the University of Rajshahi. The *A. polystachya* plant was identified (Herbarium no. 33) by the Department of Botany at the University of Rajshahi. Strains of the bacteria *E. coli* (ATCC-8739), *Pseudomonas* sp. (ATCC-27833), and *Staphylococcus* sp. (ATCC-25923), and the fungus *Lasiodiplodia theobromae* (CBS 112874) were acquired from the Microbiology Laboratory in the Department of Genetic Engineering and Biotechnology at the University of Rajshahi.

2.2. Preparation of extracts

The collected samples were washed under running tap water to remove contaminants and dust and then dried at room temperature. Finally, the dried samples were powdered with an electric grinder (Jaipan Family Mate, Mumbai, India). Methanolic extracts were prepared according to the method described by Mariswamy et al. (2011) in which 100 g of each sample was mixed with 500 mL of methanol solvent (Merck, Germany) for 5 days in an orbital shaker (Hanna, Romania). For the aqueous extracts, 100 g of each sample was crushed with a mortar and pestle. The extracts were filtered through Whatman no. 1 filter paper (Sigma-Aldrich, India) to remove debris and kept in open containers at room temperature for evaporation. The yield was 5.95 g methanolic bark extract, 4.87 g methanolic leaf extract, 4.07 g aqueous bark extract, and 4.17 g aqueous leaf extract. The prepared extracts were stored in airtight vials at 4 °C until use.

2.3. Antibacterial activity test

Antibacterial activity was tested according to the method described by Nostro et al. (2000). Whatman no. 1 filter paper was cut into 6 mm discs and sterilized. Then, starting with extracts at an adjusted final concentration of 5 mg/mL, the sterilized discs were soaked with diluted extracts at concentrations of 50, *l*00, and 150 μg/mL. Finally, 150 μl of each bacterial culture was seeded on each agar plate, and the treated discs were placed on each plate with sterile forceps. Kanamycin (Sigma-Aldrich, India) was used as a control. The plates were incubated overnight at 37 °C for observation.

2.4. Antifungal activity test

Antifungal activity was tested according to the method described by Bahraminejad et al. (2011) with some modifications. The extract concentration was adjusted to 5 mg/mL and spread at 2500 μg/mL on each potato dextrose agar (PDA) plate (Sigma-Aldrich, India). The control plates were 100% methanol and autoclaved distilled water. A 6-mm diameter fungal culture was placed at the center of each plate and incubated at normal temperature in dark conditions. After 7 days the diameter of the colony was measured. The inhibition percentage was calculated according to the formula described by Sarkar et al. (2003).

2.5. Cytotoxicity assay

An *in vitro* cytotoxicity test was performed on brine shrimp (*Artemia salina*) nauplii according to the method described by Meyer et al. (1982). Brine shrimp (Biotech Pvt. Ltd. India) were hatched at room temperature in a tank. Test tubes were prepared with extract concentrations of 25, 50, 100, 200, 300, 400, and 500 μg/mL. Then, 20 live brine shrimp nauplii were placed in each test tube with 5 mL seawater and kept at room temperature for 24 h. Finally, the LC_{50} (lethal concentration 50) was calculated by plotting the results on a linear scatter graph in Excel.

2.6. Antioxidant activity test

Antioxidant activity was tested with DPPH (2,2-Diphenyl-1-Picryl-Hydrazyl-Hydrate; Sigma-Aldrich, Bengaluru, India) in a free radical scavenging assay according to the method described by Rahman et al. (2015). The concentration of the extracts was adjusted to 50, 100, 150, 200, and 250 μg/mL by adding methanol and distilled water for methanolic and aqueous extract respectively, Then, 1.5 mL of 0.1 mM DPPH solution was added to each test tube. The samples were then incubated at room temperature for 30 min in a dark place. Finally, absorbance at 517 nm was taken using a spectrophotometer (Analytik Jena, Germany) with BHT (Sigma-Aldrich, India) as a control (Jahan et al., 2020). The percentage of scavenging was calculated according to the formula described by Mahmud et al. (2021b) and the IC_{50} (half maximal inhibitory concentration) was calculated by plotting the results on a linear scatter graph in Excel.

2.7. Evaluation of MIC

The minimal inhibitory concentration (MIC) of two plant extracts against selected microbes was tested by the tube dilution method. Test tubes of the plant extracts at concentrations of 100, 50, 25, 12.5, 6.25, 3.125, 1.56, 0.78, and 0.39 μg/mL were prepared, and 1 mL of each microbial culture was added to each test tube and incubated at 37 °C for observing microbial growth.

2.8. Observation of phytoconstituents

2.8.1. Phenolic test

The phenolic compounds were measured according to the method described by Siddhuraju and Becker (2003). Test tubes were prepared with 2 mg leaf or bark extract mixed with 2 mL distilled water, and then a 5% $FeCl_3$ (Merck, India) solution was added. The formation of a dark green color indicated the presence of phenolic compounds.

2.8.2. Flavonoids test

The flavonoids test was carried out according to the method described by Zhishen et al. (1999). Test tubes were prepared with 1 mg of each extract dissolved in 1 mL of distilled water, and then concentrated HCl (Merck, Germany) was added. The formation of a red color indicated the presence of flavonoids.

2.8.3. Alkaloids test

The alkaloids test was carried out according to the method described by Bhandari et al. (2017). Test tubes were prepared with 2 mg of each extract mixed with a few drops of Mayer's reagent (Loba, India). The formation of white or pale-yellow precipitate indicated the presence of alkaloids.

2.8.4. Terpenoids test

The terpenoids test was performed by mixing 5 mg extract samples with 2 mL of chloroform (DaeJung, Korea), and then adding 3 mL of concentrated H_2SO_4 (Merck, Germany). The formation of reddish-brown precipitate indicated the presence of terpenoids (Uddin et al., 2012).

2.8.5. Tannins test

The tannins test was performed by stirring 1 mg of each extract continuously with distilled water, and then adding 5% $FeCl_3$ (Merck, India) solution. The absence of blue-black precipitate indicated the absence of tannins (Siddhuraju and Manian, 2007).

2.8.6. Steroids test

The steroids test was performed by dissolving 1 mg of leaf and bark extract in 10 mL of chloroform and then adding an equal volume of concentrated H_2SO_4 (Merck, Germany). The formation of a red color in the upper layer indicated the presence of steroids (Senguttuvan et al., 2014).

2.9. Molecular docking study

2.9.1. Ligand preparation

The chemical compounds of *A. polystachya* (Rahman et al., 2017; Saboo et al., 2014; Wang et al., 2013) were retrieved from the PubChem database after a deep literature review (Kim et al., 2016). The compounds were extracted in 3D format and subjected to energy minimization by employing a Merck molecular force field (MMFF94).

2.9.2. Protein preparation

The protein crystal structures of *E.coli* (PDB ID: 1HNJ), *Pseudomonas* sp. (PDB ID: 1U1Z), and *Staphylococcus* sp. (PDB ID: 1JIJ) were taken from a protein data bank. The protein structures were initially cleaned and heteroatoms were removed with the aid of Pymol software (version 2.4.0) and Discovery Studio software (version 4.5.0). The cleaned proteins were energy minimized and optimized in Swiss PDB Viewer software (version 4.1) and the GROningen MOlecular Simulation (GROMOS) 431B force field was used (Spoel et al., 2005). The quality and geometry of the protein structure were evaluated from the Ramachandran plot analysis (Figure S3).

2.9.3. Molecular docking

To understand the binding dynamics of the target proteins and compounds from *Aphamixis polystachya*, a molecular docking study was carried out in the AutoDock Vina software package (version 1.1.2) (Goodsell et al., 1996; Trott and Olson, 2010). The protein structure was loaded into the software and converted into macromolecules. Thereafter, the ligand molecules were converted to PDBQT format. The center and grid box size of the docked complexes are tabulated in Table 1. Lamarckian genetic algorithms were applied to deal with ligand–protein interactions. The most favorable free binding energy and docking orientations lying within the range of 2.0 Å root-mean-square deviation (RMSD) were used to cluster the molecules and rank them accordingly. The molecular docking was performed with an energy range of 10, 20 modes, and an exhaustiveness of 8. Finally, the docked complexes were analyzed for nonbonded interactions in Pymol (DeLano, 2002) and Discovery Studio (San Diego: Accelrys Software Inc., 2012).

2.9.4. ADMET prediction

The chemical compounds that passed the docking study were subjected to absorption, distribution, metabolism, excretion, and toxicity (ADMET) filtering to identify the presence of desirable properties to be considered in a lead molecule. Therefore, the ADMETsar (http://lmmd.ecust.edu.cn › admetsar1) server was employed to calculate absorption, distribution, metabolism, excretion, and toxicity profiles using the canonical Simplified molecular-input line-entry system (SMILES) notation of the ligand molecules (Cheng et al., 2012). The PKCSM webserver (http://biosig.unimelb.edu.au › pkcsm) was employed to calculate molecules' adherence to Lipinski's rule of five (Pires et al., 2015).

Table 1
The grid box and box size of the docked pose in AutoDock Vina software package.

Protein ID	Center (Å)	Dimension (Å)
1hnj	26.1997 × 25.92 × 22.02	57.68 × 56.578 × 46.1378
1jij	−11.692 × 17.2899 × 91.74	43.90 × 66.9841 × 51.45
1u1z	16.6338 × 44.9820 × 134.04	47.78 × 41.41 × 31.86

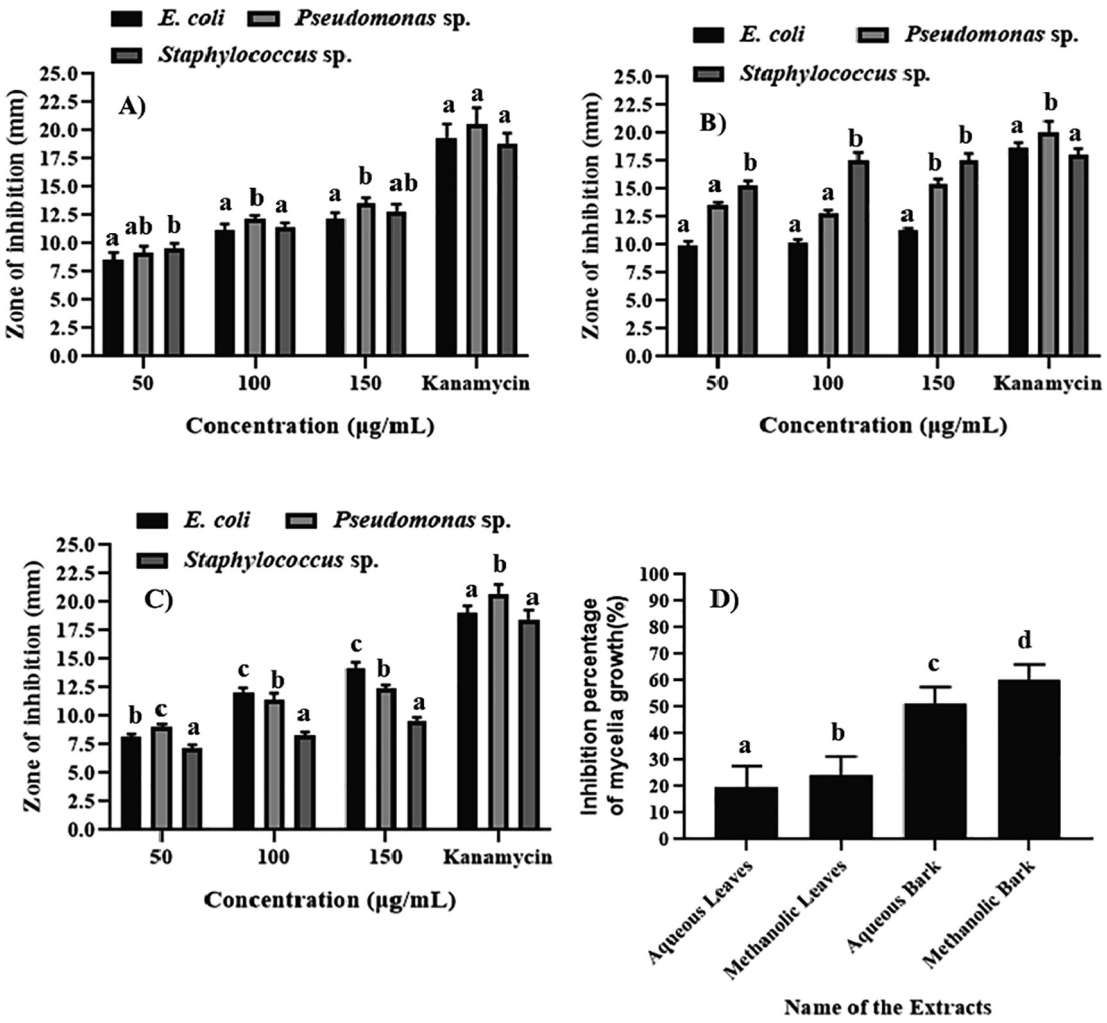

Fig. 1. Antimicrobial activities of A. polystachya leaves and bark. (**A**) methanolic extract of leaves, (**B**) and (**C**) aqueous and methanolic extract of bark, (**D**) Antifungal activity against *Lasiodiplodia theobromae*. Different significant letters indicate significant differences between mean ± SD of replications (n = 5) at a $P \leq 0.05$ significant level.

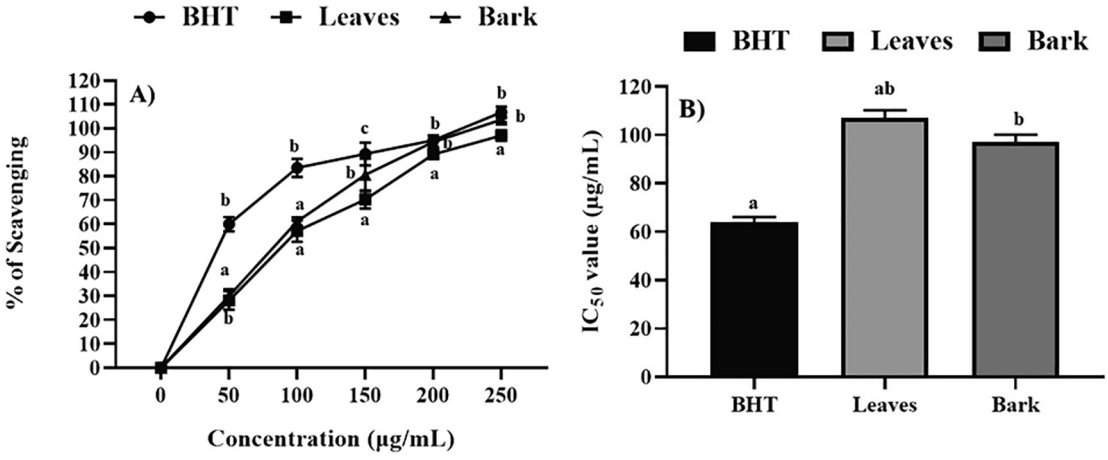

Fig. 2. The antioxidant activity of leaves and bark extracts. **(A)** Scavenging activity. **(B)** IC_{50} values of extracts with BHT standard. Different significant letters indicate significant differences between mean ± SD of replications (n = 5) at a $P \leq 0.05$ significant level.

2.9.5. Molecular dynamics

The molecular dynamics simulation study was conducted in Yet Another Scientific Artificial Reality Application (YASARA) Dynamics with the aid of the Assisted Model Building with Energy Refinement (AMBER)14 force field (Land and Humble, 2018; Wang et al., 2004). The docked complexes were initially cleaned and optimized, and the hydrogen bond network was optimized as well. The TIP3P solvation model was used with a periodic boundary condition and a cubic simulation cell was created (Harrach and Drossel, 2014). The physiological conditions were set at a pH of 7.4, 310 K, and

Table 2
Phytochemical constituents present in *A. polystachya* leaves and barks extract.

Name of phytoconstituents	Leaves Extract	Barks Extract
Phenolic	–	++
Flavonoids	+	+++
Alkaloids	–	++
Terpenoids	++	+++
Tannins	+	++
Steroids	+++	+++

Note: Here + = slightly present, ++ = moderately present, +++ = highly present, and - = absent.

0.9% NaCl (Krieger et al., 2012). The simulation time step was set at 2.0 fs. The long-range electrostatic interaction was calculated by the particle mesh Ewald (PME) method with a cutoff radius of 8.0 Å (Essmann et al., 1995). The initial energy minimization was conducted with steepest gradient algorithms (5000 cycles) by simulated annealing methods. The simulation trajectories were saved after every 100 ps and the final simulation run was conducted for 100 ns (Krieger and Vriend, 2015). The simulation trajectories were utilized to analyze the root-mean-square deviation, the solvent-accessible surface area, the radius of gyration, and hydrogen bonding (Chowdhury et al., 2020; Munia et al., 2021; Pramanik et al., 2021; Rakib et al., 2021; Uddin et al., 2021).

2.10. Statistical analysis

Graph Pad Prism (version 8.4) was used for analysis and preparation of all graph figures, in which all values are reported as the mean ± SEM (standard error of the mean). The significance levels ***p < 0.001, **p < 0.01, and *p < 0.05 of all values were evaluated with a one-way ANOVA (analysis of variance). Duncan's multiple range test (DMRT) was performed with SPSS Statistics software (version 26) with five replications.

3. Results

3.1. Antibacterial activity test

The antibacterial activity of *A. polystachya* is shown in Fig. 1. The methanolic leaf extract created an inhibition zone 12.18 ± 0.54 m m, 13.52 ± 0.54 mm, and 12.86 ± 0.62 mm in diameter against *E. coli*, *Pseudomonas* sp., and *Staphylococcus* sp., respectively (Table S1, Fig. 1, and Figure S1), while the methanolic bark extract created an inhibition zone 18.68 ± 0.67 mm, 20.10 ± 0.96 mm, and 18.60 ± 0.56 mm in diameter against *E. coli*, *Pseudomonas* sp., and *Staphylococcus* sp., respectively (Table S2, Fig. 1, and Figure S2), at a dose of 150 µg/mL. The aqueous leaf extract did not show any antibacterial activity (Table S2, Fig. 1, and Figure S1), whereas the aqueous bark extract created an inhibition zone 14.22 ± 0.50

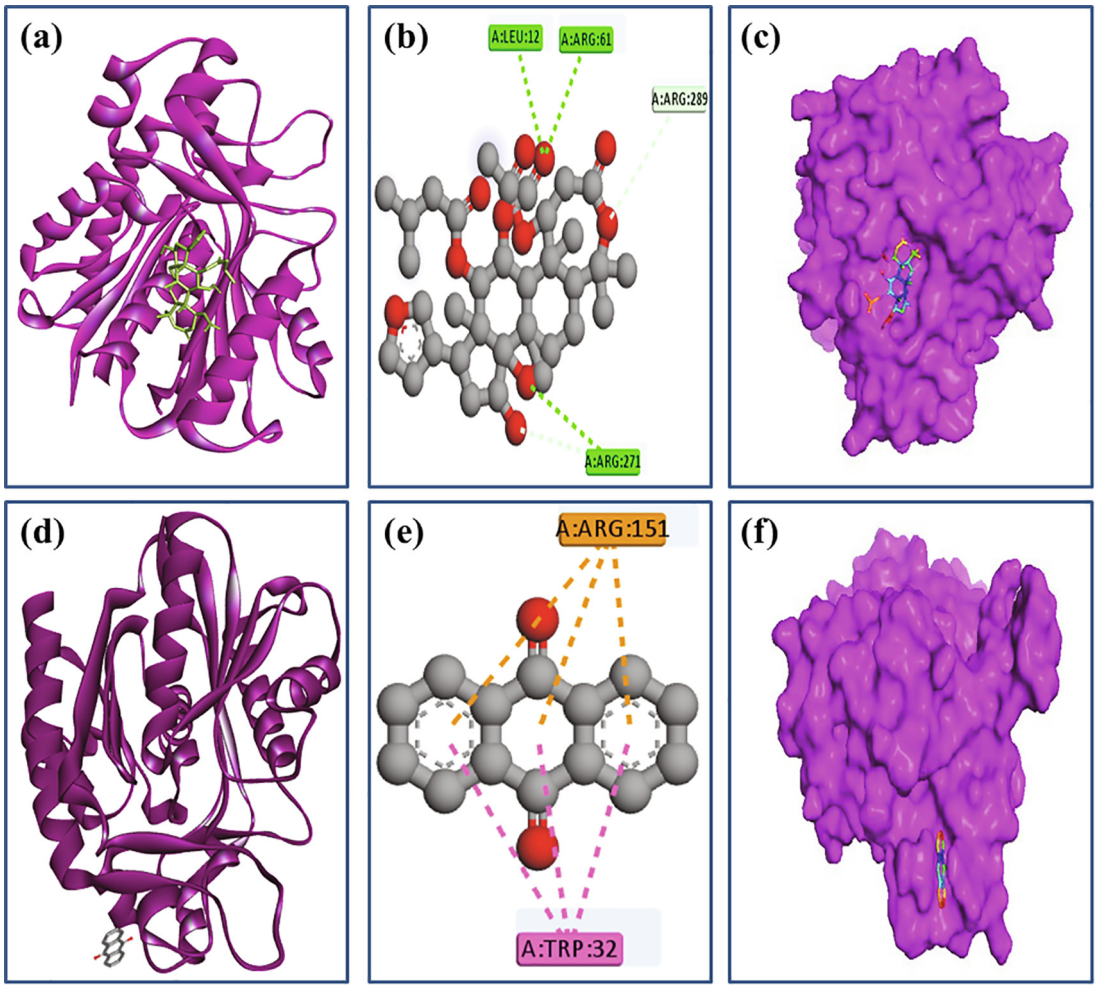

Fig. 3. Molecular docking interaction of the compounds from *A. polystachya* and FabH protein of *E. coli*. Here, a, b, c indicates cartoon view, 2D view and surface view of CID-101579586 and d, e,f indicates cartoon view, 2D view and surface view of CID-6780 respectively.

mm, 12.42 ± 0.29 mm, and 9.60 ± 0.29 mm in diameter for *E.coli*, *Pseudomonas* sp., and *Staphylococcus* sp., respectively, at a dose of 150 μg/mL (Table S2 and Fig. 1). These results indicate that the bark offers greater drug development potential than the leaves.

3.2. Cytotoxicity test

The results of the brine shrimp cytotoxicity assay (LC_{50}) for *A. polystachya* leaf and bark extracts are shown in Table S3. The LC_{50} values of methanolic and aqueous *A. polystachya* leaf extracts were 232.30 ± 4.08 μg/mL and 221.89 ± 4.24 μg/mL, respectively, whereas those of methanolic and aqueous *A. polystachya* bark extract were 251.70 ± 5.86 μg/mL and 238.25 ± 4.78 μg/mL, respectively. These results indicate a high positive correlation of bark extract concentration with brine shrimp mortality and show that *A. polystachya* bark is less toxic than the leaves.

3.3. Antioxidant screening assay

The *A. polystachya* bark extract showed DPPH free radical scavenging activity of 94.39% while the leaf extract and BHT control activity was 89.10% and 95.10%, respectively, at 200 μg/mL concentration (Fig. 2A and Table S5). The IC_{50} values of leaf extract, bark extract, and BHT were 107.14 ± 3.14 μg/mL, 97.13 ± 3.05 μg/mL, and 64.02 ± 2.01 μg/mL, respectively (Fig. 2B and Table S5). These results indicate that the bark extract had moderately high antioxidant activity compared with the leaf extract and the BHT control.

3.4. MIC test

The MIC of methanolic leaf extract was 6.25 μg/mL, 6.25 μg/mL, 12.5 μg/mL, and 12.5 μg/mL against *E. coli*, *Pseudomonas* sp., *Staphylococcus* sp., and *Lasiodiplodia theobromae*, respectively. The MIC of methanolic bark extract was 3.125 μg/mL, 1.56 μg/mL, 3.125 μg/mL, and 3.125 μg/mL, respectively (Table S6).

3.5. Phytoconstituent screening

The methanolic leaf extract showed the presence of flavonoids, terpenoids, tannins, and steroids, and the absence of phenols and alkaloids; bark extracts showed the presence of flavonoids, terpenoids, tannins, steroids, phenols, and alkaloids, and are shown in Table 2.

3.6. Molecular docking study

In this study, four phytochemicals from *A. polystachya* were screened based on lower binding energy. These ligand molecules, CID-101579586, CID-6780, CID-9548705, and CID-90785, were renamed D1, D2, D3, and D4, respectively. The D1 and D2 compounds showed higher binding affinity compared with the other chemical compounds of *A. polystachya*. The D1 and D2 compounds exhibited binding affinity energies of −7.6 Kcal/mol and −8.1 Kcal/mol, respectively. The D1 interaction with the FabH protein complex from *E. coli* was stabilized by four hydrogen bonds (Fig. 3 and Table 3) at Leu12 (2.13 Å), Arg61 (2.31 Å), Arg271 (3.09 Å), and Arg289 (2.75 Å). On the other hand, D2, which showed more binding affinity energy than D1, also had one electrostatic bond at Arg151 (3.69 Å) and one pi-pi interaction at Trp32 (3.66 Å).

The D1 compound interaction with aminoacyl-tRNA synthetases of *Staphylococcus aureus* formed three hydrogen bonds with Arg58 (2.01 Å), Asn109 (3.06 Å), and Phe306 (2.80 Å) (Fig. 4 and Table 3). This complex also featured one pi-alkyl bond at Phe273 (4.34Å). D2 showed a limited binding affinity for 1JIJ and so was not considered for this protein. However, D3 had −7.9 kcal/mol binding affinity energy for 1JIJ and created four alkyl bonds at Leu173 (4.93 Å), Ile78 (4.82 Å), Leu128 (4.39 Å), and Ile131 (5.20 Å), and one pi-alkyl bond at Phe136 (3.73 Å). D3 and FabZ have four alkyl bonds at Lys31 (4.56 Å), Leu72 (3.99 Å), Ile28 (5.21 Å), and Leu77 (5.32 Å), and two pi-alkyl bonds at Phe113 (5.43 Å), and Trp121 (4.94 Å) (Fig. 5 and Table 3). Meanwhile,

Table 3
Non-covalent interaction of the ligand molecules against three target proteins and their binding interactions; where H, A, E, PPS, PA defines the hydrogen, alkyl, Electrostatic, Pi-Pi-Stacked, and Pi-Alkyl interactions respectively. The distance of the interactions was measured in Å.

Complex	Amino Acid Residues	Bond Type	Distance(Å)	Docking Energy(Kcal/mol)
1hnj-101579586	Leu12	H	2.13	−7.6
	Arg61	H	2.31	
	Arg271	H	3.09	
	Arg289	H	2.75	
1hnj-6780	Arg151	E	3.69	−8.1
	Trp32	PPS	3.66	
1jij-9548705	Leu173	A	4.93	−7.9
	Ile78	A	4.82	
	Leu128	A	4.39	
	Ile131	A	5.20	
	Phe136	PA	3.73	
1jij-101579586	Arg58	H	2.01	−8.7
	Asn109	H	3.06	
	Phe306	H	2.80	
	Phe273	PA	4.34	
1u1z-90785	Leu72	H	2.74	−8.4
	Gly73	H	2.51	
	Ile28	A	4.86	
	Lys31	A	4.99	
	Phe113	PA	4.50	
	Trp121	PA	5.48	
1u1Z-9548705	Lys31	A	4.56	−7.9
	Leu72	A	3.99	
	Ile28	A	5.21	
	Leu77	A	5.32	
	Phe113	PA	5.43	
	Trp121	PA	4.94	

the D4 compound had the highest binding affinity energy (-8.4 Kcal/mol) of all compounds that were run against 1ULZ (Table 3). This complex had two hydrogen bonds at Leu72 (2.74 Å) and Gly73 (2.51 Å), and four hydrophobic interactions at Ile28 (4.86 Å), Lys31 (4.99 Å), Phe113 (4.50 Å), and Trp121 (5.48 Å).

3.7. Admet

The ADMET characteristics were evaluated through the ADMET-SAR webserver. Molecular weight, logP, human intestinal absorption, blood–brain barrier permeability, P-glycoprotein inhibition, carcinogenicity, AMES toxicity, and human ether-a-go-go (hERG) inhibition were checked for the ligand molecules. The results showed that, except for ligand D1, the screened ligand molecules have molecular weights lower than 500 Da (Table 4), although the molecular weight of D1 did not exceed this threshold by much. The blood–brain barrier plays a critical role in maintaining the homeostasis of the brain as it regulates the entry of ions, macromolecules, and neurotransmitters (Pimentel et al., 2020), whereas human intestinal absorption parameters can act as indicators of the bioavailability of drug candidates and are among the fundamental indicators for the preclinical evaluation of drug candidates (Wang et al., 2017). All ligand molecules showed positive results in human intestinal absorption, blood–brain barrier permeability, and P-glycoprotein inhibition. In addition, the toxicity and carcinogenicity predictions confirmed that none of the ligand molecules were likely to cause negative effects, and only D2 was anticipated to be toxic according to the AMES toxicity test. The final test assessed hERG inhibition, which plays a vital role for cardiac action potential generation; inhibition of hERG is associated with cardiac death and QT prolongation. Among the four compounds, only D2 showed potential to inhibit hERG, which suggests the other three compounds are suitable for further lab experiments.

The Lipinski rule-of-five properties were calculated to explore the drug-likeness properties of the four ligand molecules isolated from *A. polystachya*. In general, compounds need to follow the Lipinski rule to be acceptable as drugs; however, for certain drugs, such as cancer drugs, some of the rules are violated. So, violation of some Lipinski rule properties may be acceptable if the compounds possess certain other drug-likeness properties (Mahmud et al., 2021c, 2020b; Swargiary et al., 2020). However, the compounds need to have a molecular weight below 500 Da, $\leq$5H-bond donors, $\leq$10*H*-bond acceptors, and a logP $\leq$ 5 to follow the Lipinski rule. D1 had a molecular weight of over 500 Da (630.731) but it followed the other rules (Fig. 3). The other three ligand molecules (D2, D3, and D4) met the Lipinski rule of five in molecular weight, hydrogen bond donors, hydrogen bond acceptors, and logP solubility (Table 5).

3.8. Molecular dynamics

3.8.1. FabH protein complex from E. Coli

The molecular dynamics simulation study was conducted to validate the docking conformations and rigidity of the docked com-

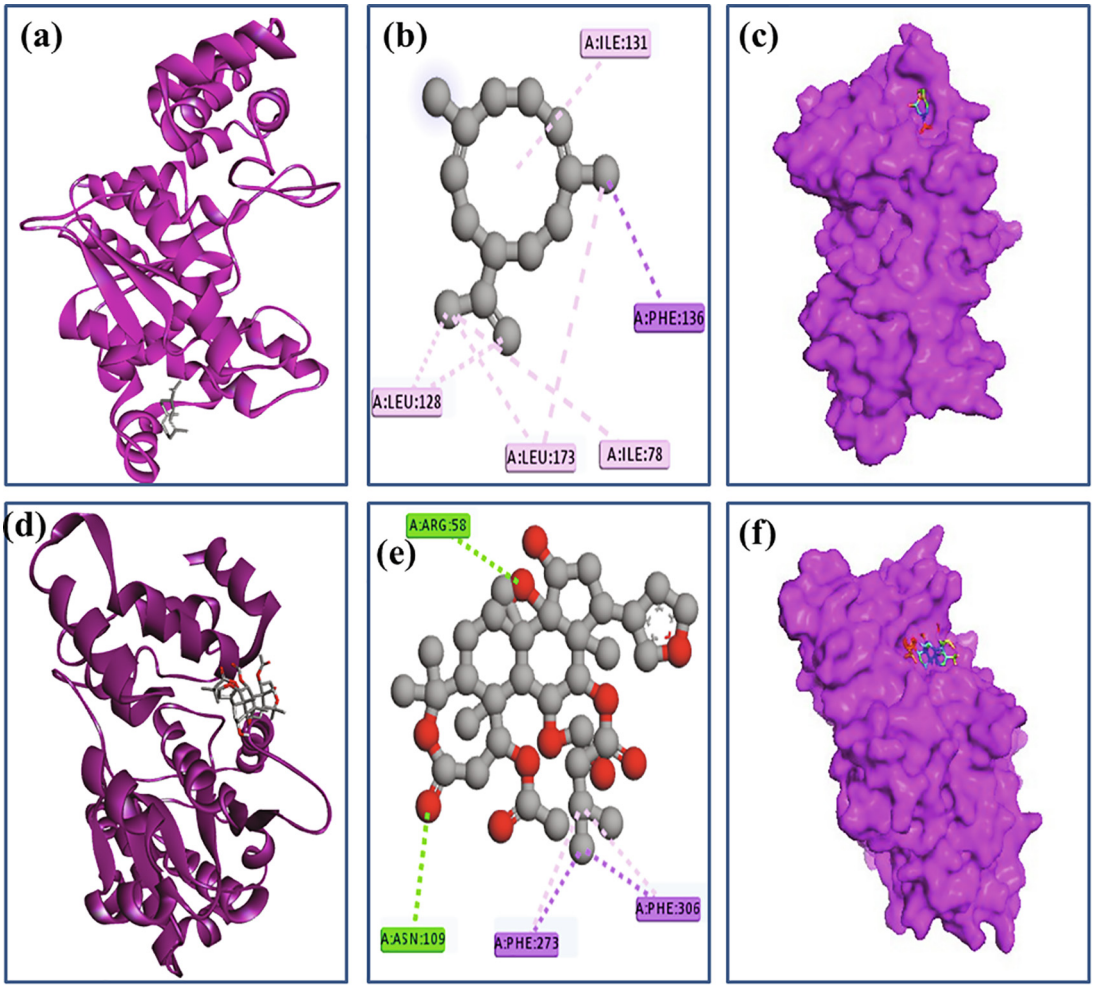

Fig. 4. Binding interaction of tRNA syntheses of *Staphylococcus aureus* and plant compounds. Here, a, b, c indicates cartoon view, 2D view and surface view of CID-101579586 and d, e, f indicates cartoon view, 2D view and surface view of CID-9548705 respectively.

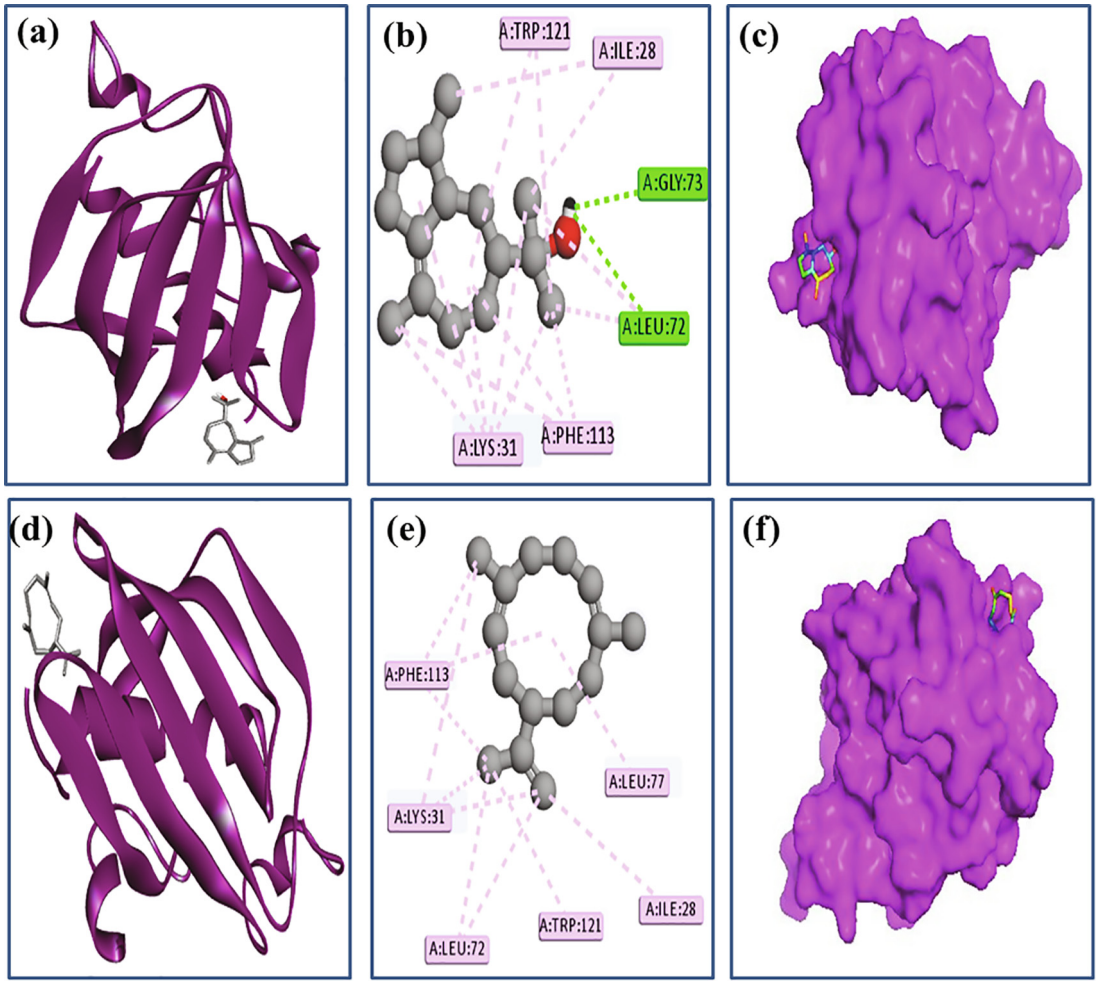

Fig. 5. Docking simulation between FabZ of *Pseudomonas aeruginosa* and plant compounds. Here, a, b, c indicates cartoon view, 2D view and surface view of CID-9548705 and d, e, f indicates cartoon view, 2D view and surface view of CID-90785 respectively.

Table 4
Pharmacological and toxicity prediction of the filtered compound from *A. polystachya* from ADMETSAR, and PKCSM tools where every compounds had almost favorable drug likeness properties.

Parameter	101579586/D1	**6780/D2**	**9548705/D3**	**90785/D4**
Molecular Weight	630.73	208.22	204.36	222.37
AlogP	4.09	2.46	5.04	3.92
Human Intestinal Absorption	0.9722(+)	0.9956(+)	0.9692(+)	0.9892(+)
Blood Brain Barrier	0.9557(+)	0.8566(+)	0.9962(+)	0.9798(+)
P-Glycoprotein Inhibitor	0.8199	0.9169	0.9428	0.9098
Carcinogenicity	0.9429(-)	0.7122(-)	0.5827(-)	0.8714(-)
AMES toxicity	0.5750(-)	0.7300(+)	0.9900(-)	0.7500(-)
Humane ither-a-go-go inhibition	0.7033(+)	0.8277(-)	0.7064(+)	0.4551(-)

Table 5
The Lipinski rule of five for best four compounds, which was calculated from the PKCSM webserver.

Parameters	101579586/D1	**6780/D2**	**9548705/D3**	**90785/D4**
Molecular Weight	630.731	208.216	204.253	222.732
LogP	4.097	2.24	5.03	3.92
Hydrogen Bond Donor	1	1	1	1
HydrogenBond Acceptors	11	2	1	1
Surface Area	263.153	92.356	94.774	99.941

plexes. The root-mean-square deviations of the C-alpha from the FabH protein complex derived from *E. coli* and the best ligand complexes are shown in Fig. 6. The D1 complex showed an increase in RMSD after 10 ns by following the upward movements, whereas the D2 complex showed the opposite trend. This might be due to the conformational variability of D1 complexes after 10 ns. However, both the D1 and D2 complexes maintained a stable RMSD after 20 ns for the rest of the simulation period. However, the

solvent-accessible surface area (SASA) of the complexes showed slightly different trends. The D1 complexes had higher SASA while the D2 complexes had lower SASA. This might be due to the increased surface area of the D1 complex. The radius of gyration (Rg) profile from the simulation trajectories was assessed to examine the degree of the flexibility of the complex. The figure shows that the D1 and D2 complexes had steady Rg profiles, indicating a lower degree of flexibility in the complex. The hydrogen bonds of the drug-protein complex determine the stability and firmness of the complex. The figure indicates that the hydrogen bonds of both complexes were in a less volatile state.

3.8.2. Aminoacyl-tRNA synthetases of Staphylococcus aureus

The RMSD of the aminoacyl-tRNA synthetase complexes was upward-trending from the beginning of the simulation, which might be due to the conformational variations of the complexes. However, the RMSD trend stabilized in the D1 and D3 complexes after they reached a steady state, and these maintained a similar profile until the end of the simulation period. The overall RMSD trend of the two complexes was below 2.5 Å, which demonstrates the stability of the complexes. The higher SASA is due to the extension of the surface area whereas the lower SASA correlates with the condensed nature of the protein systems. Fig. 7 indicates that the D3 complex had higher SASA upon ligand binding, and this might be due to the amplified flexibility of the protein-drug complex. The D1 complex had the lower SASA profile. The Rg profiles of the D1 and D3 complexes were similar, but these deviated between 20 ns and 40 ns. This indicates folding and a change in the conformation of the complexes. However, the two complexes had lower degrees of flexibility as measured by Rg over the rest of the simulation, which confirms the stable and rigid profile of the simulated complexes. The hydrogen bonds of both the D1 and D3 complexes were similar and did not change during the simulation.

3.8.3. (3R)-hydroxyacyl-ACP dehydratase (FabZ) from Pseudomonas sp.

The RMSD profiles from the (3R)-hydroxyacyl-ACP dehydratase (FabZ) complexes (D3 and D4) were also assessed to validate the docking study. Both complexes formed with this protein had lower RMSD from the beginning but experienced an intermittent increase after 40 ns (Fig. 8). Both the D3 and D4 complexes had stable trends after 40 ns until the last phase of the simulation, which assessed the rigidity of the complexes. The SASA of the D3 and D4 complexes trended similarly after 40 ns and had a stable profile as well. The Rg profiles of the two complexes differ slightly from the others, which demonstrates the more labile and mobile nature of the D3 and D4 complexes. The hydrogen bond pattern of both complexes demonstrates their stable state.

4. Discussion

Plant-derived phytochemicals have recently garnered more interest as a source of novel drug candidates and pharmaceutical therapeutics against infectious diseases (Zhang et al., 2013). Many plant parts exhibit antimicrobial and antioxidant activities (Beuchat, 1994; Hara-Kudo et al., 2004; Stewart et al., 1998). The results of this research confirm the potential medicinal use of *A. polystachya* bark, which can be considered a good source of medicine due to its considerable application in complaints such as respiratory, urological, gastrointestinal, liver, and spleen disorders.

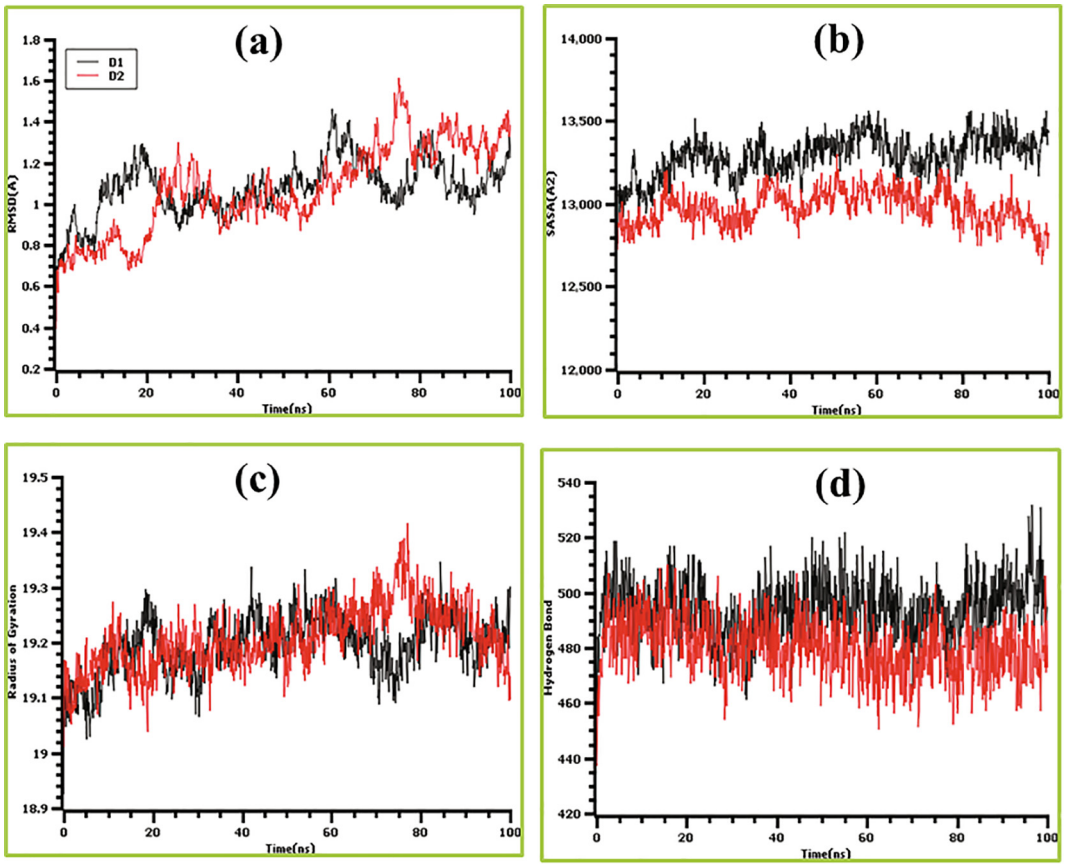

Fig. 6. The molecular dynamics simulation study of FabH protein of *E. coli* and D1 and D2 complexes, (a) root mean square deviation, (b) solvent accessible surface area, (c) radius of gyration, (d) hydrogen bond.

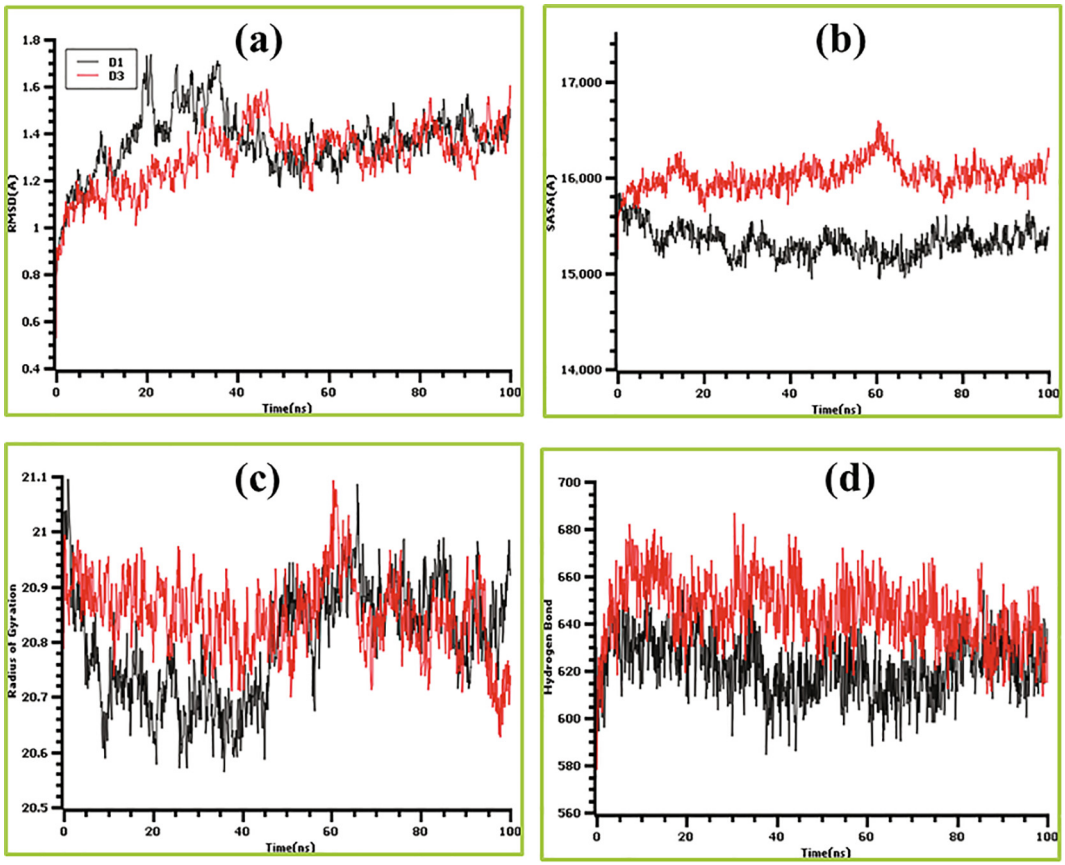

Fig. 7. The simulation study of tRNA syntheses of *Staphylococcus aureus* and D1, D3 complexes where a, b, c, d indicates (a) root mean square deviations, (b) solvent accessible surface area, (c) radius of gyration, and (d) hydrogen bond respectively.

The antimicrobial activity of *A. polystachya* leaf and bark extracts has been tested against four microbial stains, but only bark extracts exhibited significant antimicrobial activity against the tested microorganisms (Fig. 1).

The presence of phytoconstituents such as phenols, flavonoids, terpenoids, tannins, and steroids are usually important indicators that a plant extract's antioxidant properties may be able to inhibit the enzymes that are essential for microbial replication (Das et al., 2018). A DPPH free radical scavenging assay is the preferred measurement of the antioxidant activity of plant compounds (Choi et al., 2000), and specific compounds exhibit anticancer activity (XiaoPing et al., 2009). The present investigation also indicated that the bark extract of *A. polystachya* showed high antioxidant activity (Fig. 2A). A study also reported that some plants had a less toxic effect on brine shrimp in lethality assays (Carballo et al., 2002), a claim that is significantly supported by the present investigation. The bark extracts showed lower toxicity than leaves (Table S3 and S4), and the mortality rate increased according to the increase in the concentration. As the LC_{50} was high for both bark extracts, these can be considered biological agents with high potential for molecular docking studies.

Plant antioxidants can protect cells from damage by free radicals and molecular docking studies are used to find the interaction dynamics of a protein complex. These two studies were integrated to identify the pharmacological properties of the bark extract. Antioxidant activity can be checked via molecular docking under in silico conditions, but in this study, the antioxidant activity was assessed under lab conditions and molecular docking was used only to assess the properties of phytochemicals derived from *A. polystachya* bark against target proteins. The results suggest that the bark extract has higher antioxidant and antimicrobial activity than the leaf extract with less cytotoxicity. Thus *A. polystachya* bark extracts show high potential as sources for developing drugs to treat antibiotic-resistant microbes.

Furthermore, a combination of molecular docking and molecular dynamics study enables the identification of potent inhibitors from diverse datasets. This study provides crucial understanding of ligand–protein interactions, along with the target binding sites (Mahmud et al., 2021d). Moreover, multiple studies were conducted in search of effective inhibitors against target proteins due to advancements in the development of computational algorithms as well as the exploration of the specific interaction dynamics of ligand–protein complexes (DaRoch, n.d.; Eissa et al., 2021; Rahman et al., 2020).

Bacterial fatty acid synthesis and the elongation of fatty acids can be initiated by FabH, one of the beta-ketoacyl-acyl-carrier protein synthases (Cronan Jr. and Rock, 2008; Heath and Rock, 1996; Tsay et al., 1992). In the development of antibacterial and antimicrobial drugs, FabI (enoyl-ACP reductase) and FabH have been targeted especially; isoniazid for tuberculosis operates in this way, as do cerulenin and thiolactomycin (Banerjee et al., 1994; Mdluli et al., 1998; Moche et al., 1999; Rozwarski et al., 1998). The FabH protein of *E. coli* is comprised of two monomeric structures with N terminal and C terminal domains where acetyl-CoA binds in the substrate binding zone (Fig. 3). The CoA adenosine ring between Arg151 and Trp32 and a hydrogen bond between Thr28 and Arg151 were observed. In our docking study, the D2 compound created a nonbonded interaction with the FabH protein in these active grooves, which might be a source of inhibition. These hydrophobic interactions were supported by the interaction of

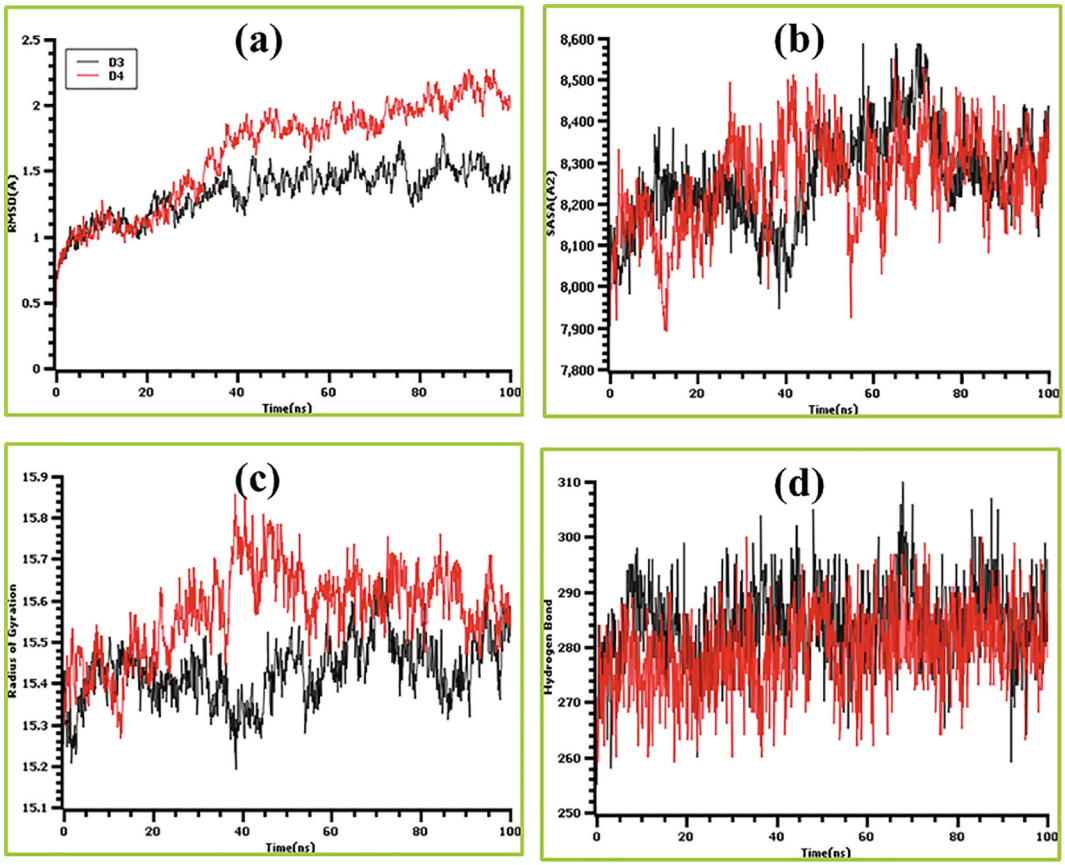

Fig. 8. The dynamics simulation study of the FabZ of *Pseudomonas aeruginosa* and D3 and D4 complexes, where (a) root mean square deviation, (b) solvent accessible surface area, (c) radius of gyration, (d) hydrogen bond.

FabH and CoA where similar binding patterns were observed (Qiu et al., 2001a).

On the other hand, charged tRNA production can be initiated by aminoacyl-tRNA synthetase-driven protein synthesis. During this process, an amino acid is bonded to an ATP molecule to create a stable aminoacyl-adenylate intermediate, which ultimately binds to its cognate tRNA and forms a charged tRNA molecule. This protein is a potential target for the antibacterial activity of phytochemicals and drug molecules in *Staphylococcus aureus* (Fersht et al., 1988; Schimmel et al., 1998). Previous crystal structure studies suggest that the alpha-helical domain of this protein consists of five helices and the alpha/beta domain contains a six-stranded beta-sheet with an active site cleft. The co-crystalized ligand molecules created hydrophobic bonds with Tyr169, Asp78, Gln173, Asp176, Tyr34, and Lys82 which aligns with the observed binding interaction between D3 and tRNA synthetases (Fig. 4) of *Staphylococcus aureus* (Brick and Blow, 1987; Brown et al., 1987). Moreover, the binding of SB-284485 and the crystal structure also confirmed similar interactions (Qiu et al., 2001b).

The fatty acid biosynthesis system is required for the formation of bacterial membranes, which makes it an attractive target for antibacterial drugs. This fatty acid biosynthesis process is catalyzed by FabZ in *Pseudomonas aeruginosa* (Kimber et al., 2004). Both D3 and D4 compounds interacted with the active sites of FabZ, inhibiting the targeted FabZ protein (Fig. 5).

The pharmacological properties of drug candidates must be assessed appropriately to be approved for further clinical experiments but the expense of clinical experiments and laboratory use makes it difficult to evaluate drug molecules vigorously. *In silico* ADMET prediction is a suitable tool to screen the likely compounds based on desirable pharmacological characteristics (Mahmud et al., 2020a, 2020b). In the present study, all chosen compounds possess favorable pharmacological properties, although some deviations from Lipinski's rule of five were observed.

5. Conclusion

Plants have become a useful source of treatment due to their wide availability, reduced side effects, and increased specificity compared with synthetic compounds. To treat antibiotic-resistant bacterial infections, *A. polystachya* bark extracts may be potent inhibitors of select stains. The antioxidant and lethality assessments of the bark extracts also showed significant effects with a low risk of negative effects, and the isolated compounds were able to bind with the tested microbial strains. Through molecular docking assays, aphanalide A, anthraquinone, germacrene a, and bulnesol were found to have the highest target binding affinities for these strains. The structural rigidity of the complexes formed was also confirmed by molecular dynamics simulations. This study may help future researchers identify an effective drug for the control of *E. coli, Pseudomonas* sp., and *Staphylococcus* sp. infections. Further experiments should explore the safety profiles of the candidate components derived from *A. polystachya* bark.

Funding

This research did not receive any grant.

Declaration of Competing Interest

The authors declare that they have no known competing financial interests or personal relationships that could have appeared to influence the work reported in this paper.

Acknowledgements

This research work was internally funded by the Microbiology Laboratory, Department of Genetic Engineering and Biotechnology, University of Rajshahi, 6205, Bangladesh. The authors acknowledge Almighty Allah and all those who have helped and supported us along the way.

Appendix A. Supplementary material

Supplementary data to this article can be found online at https://doi.org/10.1016/j.sjbs.2021.07.032.

References

Amenu, D., 2014. Antimicrobial Activity of Medicinal Plant Extracts and Their Synergistic Effect on Some Selected Pathogens. Am. J. Ethnomed. 1 (1), 18–29.
Bahraminejad, S., Abbasi, S., Fazlali, M., 2011. In vitro antifungal activity of 63 Iranian plant species against three different plant pathogenic fungi. Afr. J. Biotechnol. https://doi.org/10.5897/AJB11.1203.
Banerjee, A., Dubnau, E., Quemard, A., Balasubramanian, V., Um, K.S., Wilson, T., Collins, D., De Lisle, G., Jacobs, W.R., 1994. inhA, a gene encoding a target for isoniazid and ethionamide in Mycobacterium tuberculosis. Science (80-.). 263, 227–230.
Baravalia, Y., Vaghasiya, Y., Chanda, S., 2012. Brine shrimp cytotoxicity, anti-inflammatory and analgesic properties of Woodfordia fruticosa Kurz flowers. Iran. J. Pharm. Res. 11, 851–861. https://doi.org/10.22037/IJPR.2012.1111.
Beuchat, L.R., 1994. Antimicrobial properties of spices and their essential oils. Nat. Antimicrob. Syst. Food Preserv. 12, 257–262.
Bhandari, J., Muhammad, B., Thapa, P., Shrestha, B.G., 2017. Study of phytochemical, anti-microbial, anti-oxidant, and anti-cancer properties of Allium wallichii. BMC Complement. Altern. Med. 17, 102.
Bhavsar, A.P., Guttman, J.A., Finlay, B.B., 2007. Manipulation of host-cell pathways by bacterial pathogens. Nature 449 (7164), 827–834. https://doi.org/10.1038/nature06247.
Brick, P., Blow, D.M., 1987. Crystal structure of a deletion mutant of a tyrosyl-tRNA synthetase complexed with tyrosine. J. Mol. Biol. 194 (2), 287–297.
Brouwer, S., Barnett, T.C., Rivera-Hernandez, T., Rohde, M., Walker, M.J., 2016. Streptococcus pyogenes adhesion and colonization. FEBS Lett. 590 (21), 3739–3757. https://doi.org/10.1002/feb2.2016.590.issue-2110.1002/1873-3468.12254.
Brown, K.A., Brick, P., Blow, D.M., 1987. Structure of a mutant of tyrosyl-tRNA synthetase with enhanced catalytic properties. Nature 326 (6111), 416–418.
Carballo, J.L., Hernández-Inda, Z.L., Pérez, P., García-Grávalos, M.D., 2002. A comparison between two brine shrimp assays to detect in vitro cytotoxicity in marine natural products. BMC Biotechnol. 2. https://doi.org/10.1186/1472-6570-2-17.
Carocho, M., Ferreira, I.C.F.R., 2013. A review on antioxidants, prooxidants and related controversy: Natural and synthetic compounds, screening and analysis methodologies and future perspectives. Food Chem. Toxicol. 51, 15–25. https://doi.org/10.1016/j.fct.2012.09.021.
Cheng, F., Li, W., Zhou, Y., Shen, J., Wu, Z., Liu, G., Lee, P.W., Tang, Y., 2012. AdmetSAR: A comprehensive source and free tool for assessment of chemical ADMET properties. J. Chem. Inf. Model. 52 (11), 3099–3105. https://doi.org/10.1021/ci300367a.
Choi, H.S., Sun Song, H., Ukeda, H., Sawamura, M., 2000. Radical-scavenging activities of citrus essential oils and their components: Detection using 1,1-diphenyl-2-picrylhydrazyl. J. Agric. Food Chem. 48, 4156–4161. https://doi.org/10.1021/jf000227d.
Chowdhury, K.H., Chowdhury, M.R., Mahmud, S., Tareq, A.M., Hanif, N.B., Banu, N., Reza, A.S.M.A., Emran, T.B., Simal-Gandara, J., 2020. Drug Repurposing Approach against Novel Coronavirus Disease (COVID-19) through Virtual Screening Targeting SARS-CoV-2 Main Protease. Biology (Basel). 10, 2. https://doi.org/10.3390/biology10010002.
Cronan Jr, J.E., Rock, C.O., Stewart, V., Begley, T.J., 2008. Biosynthesis of membrane lipids. EcoSal Plus 3 (1). https://doi.org/10.1128/ecosalplus.3.6.4.
Das, S.K., Samantaray, D., Mahapatra, A., Pal, N., Munda, R., Thatoi, H., 2018. Pharmacological activities of leaf and bark extracts of a medicinal mangrove plant Avicennia officinalis L. Clin. Phytoscience 4 (1). https://doi.org/10.1186/s40816-018-0072-0.
DeLano, W.L., 2002. Pymol: An open-source molecular graphics tool. CCP4 Newsl. Protein Crystallogr. 40 (1), 82–92.
Djeussi, D.E., Noumedem, J.AK., Seukep, J.A., Fankam, A.G., Voukeng, I.K., Tankeo, S. B., Nkuete, A.HL., Kuete, V., 2013. Antibacterial activities of selected edible plants extracts against multidrug-resistant Gram-negative bacteria. BMC Complement. Altern. Med. 13 (1). https://doi.org/10.1186/1472-6882-13-164.
Duraipandiyan, V., Ayyanar, M., Ignacimuthu, S., 2006. Antimicrobial activity of some ethnomedicinal plants used by Paliyar tribe from Tamil Nadu, India. BMC Complement. Altern. Med. 6 (1). https://doi.org/10.1186/1472-6882-6-35.
Eissa, I.H., Ibrahim, M.K., Metwaly, A.M., Belal, A., Mehany, A.B.M., Abdelhady, A.A., Elhendawy, M.A., Radwan, M.M., ElSohly, M.A., Mahdy, H.A., 2021. Design, molecular docking, in vitro, and in vivo studies of new quinazolin-4(3H)-ones as VEGFR-2 inhibitors with potential activity against hepatocellular carcinoma. Bioorg. Chem. 107, 104532. https://doi.org/10.1016/j.bioorg.2020.104532.
Essmann, U., Perera, L., Berkowitz, M.L., Darden, T., Lee, H., Pedersen, L.G., 1995. A smooth particle mesh Ewald method. J. Chem. Phys. 103 (19), 8577–8593. https://doi.org/10.1063/1.470117.
Fersht, A.R., Knill-Jones, J.W., Bedouelle, H., Winter, G., 1988. Reconstruction by site-directed mutagenesis of the transition state for the activation of tyrosine by the tyrosyl-tRNA synthetase: a mobile loop envelopes the transition state in an induced-fit mechanism. Biochemistry 27 (5), 1581–1587.
Francine, U., Jeannette, U., Jean Pierre, R., 2015. Assessment of antibacterial activity of Neem plant (Azadirachta indica) on Staphylococcus aureus and Escherichia coli. J. Med. Plants Stud. JMPS 85, 85–91.
Franklin, D., 2003. Antimicrobial resistance : The example of Staphylococcus aureus. J. Clin. Invest. 111, 1265–1273.
Gayathri Devi, S., Sangeetha, S., Mary Shoba Das, C., 2013. Comparative evaluation of phytochemicals and antioxidant potential of Cleome viscose and Trichodesma indicum. Int. J. Pharm. Sci. Rev. Res. 23, 253–258.
Goodsell, D.S., Morris, G.M., Olson, A.J., 1996. Automated docking of flexible ligands: applications of AutoDock. J. Mol. Recognit. 9 (1), 1–5.
Hara-Kudo, Y., Kobayashi, A., Sugita-Konishi, Y., Kondo, K., 2004. Antibacterial activity of plants used in cooking for aroma and taste. J. Food Prot. 67, 2820–2824. https://doi.org/10.4315/0362-028X-67.12.2820.
Harrach, M.F., Drossel, B., 2014. Structure and dynamics of TIP3P, TIP4P, and TIP5P water near smooth and atomistic walls of different hydroaffinity. J. Chem. Phys. 140 (17), 174501. https://doi.org/10.1063/1.4872239.
Heath, R.J., Rock, C.O., 1996. Regulation of fatty acid elongation and initiation by acyl-acyl carrier protein in Escherichia coli. J. Biol. Chem. 271 (4), 1833–1836. https://doi.org/10.1074/jbc.271.4.1833.
Jahan, I., Tona, M.R., Sharmin, S., Sayeed, M.A., Tania, F.Z., Paul, A., Chy, M.N.U., Rakib, A., Emran, T.B., Simal-Gandara, J., 2020. GC-MS phytochemical profiling, pharmacological properties, and in silico studies of chukrasia velutina leaves: A novel source for bioactive agents. Molecules 25 (15), 3536. https://doi.org/10.3390/molecules25153536.
Joana Gil-Chávez, G., Villa, José.A., Fernando Ayala-Zavala, J., Basilio Heredia, J., Sepulveda, D., Yahia, E.M., González-Aguilar, G.A., 2013. Technologies for Extraction and Production of Bioactive Compounds to be Used as Nutraceuticals and Food Ingredients: An Overview. Compr. Rev. Food Sci. Food Saf. 12 (1), 5–23. https://doi.org/10.1111/crf3.2013.12.issue-110.1111/1541-4337.12005.
Kaur, G.J., Arora, D.S., 2009. Antibacterial and phytochemical screening of Anethum graveolens Foeniculum vulgare and Trachyspermum ammi. BMC Complement. Altern. Med. https://doi.org/10.1186/1472-6882-9-30.
Khademi, H., Malekzadeh, R., Pourshams, A., Jafari, E., Salahi, R., Semnani, S., Abaie, B., Islami, F., Nasseri-Moghaddam, S., Etemadi, A., Byrnes, G., Abnet, C.C., Dawsey, S.M., Day, N.E., Pharoah, P.D., Boffetta, P., Brennan, P., Kamangar, F., 2012. Opium use and mortality in Golestan Cohort Study: prospective cohort study of 50,000 adults in Iran. BMJ. https://doi.org/10.1136/bmj.e2502.
Kim, S., Thiessen, P.A., Bolton, E.E., Chen, J., Fu, G., Gindulyte, A., Han, L., He, J., He, S., Shoemaker, B.A., Wang, J., Yu, B., Zhang, J., Bryant, S.H., 2016. PubChem substance and compound databases. Nucleic Acids Res. 44 (D1), D1202–D1213.
Kimber, M.S., Martin, F., Lu, Y., Houston, S., Vedadi, M., Dharamsi, A., Fiebig, K.M., Schmid, M., Rock, C.O., 2004. The structure of (3R)-hydroxyacyl-acyl carrier protein dehydratase (FabZ) from Pseudomonas aeruginosa. J. Biol. Chem. 279 (50), 52593–52602.
Krieger, E., Dunbrack, R.L., Hooft, R.W.W., Krieger, B., 2012. Assignment of protonation states in proteins and ligands: Combining pK a prediction with hydrogen bonding network optimization. Methods Mol. Biol. 819, 405–421. https://doi.org/10.1007/978-1-61779-465-0_25.
Krieger, E., Vriend, G., 2015. New ways to boost molecular dynamics simulations. J. Comput. Chem. 36 (13), 996–1007. https://doi.org/10.1002/jcc.v36.1310.1002/jcc.23899.
Land, H., Humble, M.S., 2018. YASARA: A tool to obtain structural guidance in biocatalytic investigations. Methods Mol. Biol. 1685, 43–67. https://doi.org/10.1007/978-1-4939-7366-8_4.
Liguori, I., Russo, G., Curcio, F., Bulli, G., Aran, L., Della-Morte, D., Gargiulo, G., Testa, G., Cacciatore, F., Bonaduce, D., Abete, P., 2018. Oxidative stress, aging, and diseases. Clin. Interv. Aging 13, 757–772. https://doi.org/10.2147/CIA.S158513.
Lushchak, V.I., 2014. Free radicals, reactive oxygen species, oxidative stress and its classification. Biol. Interact Chem. https://doi.org/10.1016/j.cbi.2014.10.016.
Mahesh, B., Satish, S., 2008. Antimicrobial Activity of Some Important Medicinal Plant Against Plant and Human Pathogens. World J. Agric. Sci. 4, 839–843.
Mahmud, S., Paul, G.K., Afroze, M., Islam, S., Gupt, S.B.R., Razu, M.H., Biswas, S., Zaman, S., Uddin, M.S., Khan, M., Cacciola, N.A., Emran, T.B., Saleh, M.A., Capasso, R., Simal-Gandara, J., 2021a. Efficacy of phytochemicals derived from avicennia officinalis for the management of covid-19: A combined in silico and

biochemical study. Molecules 26 (8), 2210. https://doi.org/10.3390/molecules26082210.
Mahmud, S., Paul, G.K., Afroze, M., Islam, S., Gupt, S.B.R., Razu, M.H., Biswas, S., Zaman, S., Uddin, M.S., Khan, M., Cacciola, N.A., Bin Emran, T., Saleh, M.A., Capasso, R., Simal-Gandara, J., 2021b. Efficacy of Phytochemicals Derived from Avicennia officinalis for the Management of COVID-19: A Combined In Silico and Biochemical Study. Molecules 26, 2210. https://doi.org/10.3390/molecules26082210.
Mahmud, S., Rahman, E., Nain, Z., Billah, M., Karmokar, S., Mohanto, S.C., Paul, G.K., Amin, A., Acharjee, U.K., Saleh, M.A., 2020a. Computational Discovery of Plant-Based Inhibitors against Human Carbonic Anhydrase IX and Molecular Dynamics Simulation. J. Biomol. Struct. Dyn., 20–21 https://doi.org/10.1080/07391102.2020.1753579.
Mahmud, S., Uddin, M.A.R., Paul, G.K., Shimu, M.S.S., Islam, S., Rahman, E., Islam, A., Islam, M.S., Promi, M.M., Emran, T Bin, Saleh, M.A., 2021c. Virtual screening and molecular dynamics simulation study of plant-derived compounds to identify potential inhibitors of main protease from SARS-CoV-2. Bioinform. Brief. https://doi.org/10.1093/bib/bbaa428.
Mahmud, S., Uddin, M.A.R., Zaman, M., Sujon, K.M., Rahman, M.E., Shehab, M.N., Islam, A., Alom, M.W., Amin, A., Akash, A.S., Saleh, M.A., 2020b. Molecular docking and dynamics study of natural compound for potential inhibition of main protease of SARS-CoV-2. J. Biomol. Struct. Dyn. https://doi.org/10.1080/07391102.2020.1796808.
Manilal, A., Sujith, S., Kiran, G.S., Selvin, J., Shakir, C., 2009. Cytotoxic Potentials of Red Alga, Laurencia brandenii Collected from the Indian Coast. Glob. J. Pharmacol. 3, 90–94.
Mariswamy, Y., Gnaraj, W.E., Johnson, M., 2011. Chromatographic finger print analysis of steroids in Aerva lanata L by HPTLC technique. Asian Pac. J. Trop. Biomed. 1 (6), 428–433. https://doi.org/10.1016/S2221-1691(11)60094-4.
Mdluli, K., Slayden, R.A., Zhu, Y., Ramaswamy, S., Pan, X., Mead, D., Crane, D.D., Musser, J.M., Barry, C.E., 1998. Inhibition of a Mycobacterium tuberculosis β-ketoacyl ACP synthase by isoniazid. Science (80-) 280, 1607–1610.
Meyer, B., Ferrigni, N., Putnam, J., Jacobsen, L., Nichols, D., McLaughlin, J., 1982. Brine shrimp: a convenient general bioassay for active plant constituents. Planta Med. 45 (05), 31–34.
Moche, M., Schneider, G., Edwards, P., Dehesh, K., Lindqvist, Y., 1999. Structure of the complex between the antibiotic cerulenin and its target, β-ketoacyl-acyl carrier protein synthase. J. Biol. Chem. 274 (10), 6031–6034.
Munia, M., Mahmud, S., Mohasin, M., Kibria, K.M.K., 2021. In Silico design of an epitope-based vaccine against Choline binding protein A of Streptococcus pneumoniae. Inform. Med. Unlocked 23, 100546. https://doi.org/10.1016/j.imu.2021.100546.
Nostro, A., Germano, M.P., D'Angelo, V., Marino, A., Cannatelli, M.A., 2000. Extraction methods and bioautography for evaluation of medicinal plant antimicrobial activity. Lett. Appl. Microbiol. 30 (5), 379–384. https://doi.org/10.1046/j.1472-765x.2000.00731.x.
Pendleton, J.N., Gorman, S.P., Gilmore, B.F., 2013. Clinical relevance of the ESKAPE pathogens. Anti. Infect. Ther Expert Rev. https://doi.org/10.1586/eri.13.12.
Pimentel, E., Sivalingam, K., Doke, M., Samikkannu, T., 2020. Effects of Drugs of Abuse on the Blood-Brain Barrier: A Brief Overview. Front. Neurosci. 14. https://doi.org/10.3389/fnins.2020.00513.
Pires, D.E.V., Blundell, T.L., Ascher, D.B., 2015. pkCSM: Predicting small-molecule pharmacokinetic and toxicity properties using graph-based signatures. J. Med. Chem. 58, 4066–4072. https://doi.org/10.1021/acs.jmedchem.5b00104.
Pisutthanan, S., Plianbangchang, P., Pisutthanan, N., Ruanruay, S., Muanrit, O., 2004. Brine Shrimp Lethality Activity of Thai Medicinal Plants in the Family Meliaceae. Naresuan Univ. J. 12, 13–18.
Poojary, S., 2020. Role of Bioinformatics, Computational Biology and Computer Technologies in Combating COVID-19 Virus-a Review. Int. J. Biotech Trends Technol. 10, 26–30. https://doi.org/10.14445/22490183/ijbtt-v10i2p605.
Poonkothai, M., Saravanan, M., 2008. Antibacterial activity of Aegle marmelos against leaf, bark and fruit extracts. Anc. Sci. Life 27, 15–18.
Pramanik, S.K., Mahmud, S., Paul, G.K., Jabin, T., Naher, K., Uddin, M.S., Zaman, S., Saleh, M.A., 2021. Fermentation optimization of cellulase production from sugarcane bagasse by Bacillus pseudomycoides and molecular modeling study of cellulase. Curr. Res. Microb. Sci. 2, 100013. https://doi.org/10.1016/j.crmicr.2020.100013.
Prasad, R., Swamy, V.S., 2013. Antibacterial Activity of Silver Nanoparticles Synthesized by Bark Extract of Syzygium cumini. J. Nanoparticles 2013, 1–6. https://doi.org/10.1155/2013/431218.
Qiu, X., Janson, C.A., Smith, W.W., Green, S.M., McDevitt, P., Johanson, K., Carter, P., Hibbs, M., Lewis, C., Chalker, A., Fosberry, A., Lalonde, J., Berge, J., Brown, P., Houge-Frydrych, C.S.V., Jarvest, R.L., 2001a. Crystal structure of Staphylococcus aureus tyrosyl-tRNA synthetase in complex with a class of potent and specific inhibitors. Protein Sci. 10 (10), 2008–2016. https://doi.org/10.1110/(ISSN)1469-896X10.1110/ps.18001.
Qiu, X., Janson, C.A., Smith, W.W., Head, M., Lonsdale, J., Konstantinidis, A.K., 2001b. Refined structures of β-ketoacyl-acyl carrier protein synthase III. J. Mol. Biol. 307 (1), 341–356.
Rahman, M., Browne, J.J., Van Crugten, J., Hasan, M.F., Liu, L., Barkla, B.J., 2020. In Silico, Molecular Docking and In Vitro Antimicrobial Activity of the Major Rapeseed Seed Storage Proteins. Front. Pharmacol. 11. https://doi.org/10.3389/fphar.2020.01340.
Rahman, M.M., Islam, M.B., Biswas, M., Khurshid Alam, A.H.M., 2015. In vitro antioxidant and free radical scavenging activity of different parts of Tabebuia pallida growing in Bangladesh. BMC Res. Notes. https://doi.org/10.1186/s13104-015-1618-6.
Rahman, M.S., Ahad, A., Kumar Saha, S., Hong, J., Kim, K.-H., 2017. Antibacterial and phytochemical properties of Aphanamixis polystachya essential oil. Repository. Hanyang.Ac.Kr 30, 113–121.
Rakib, A., Nain, Z., Sami, S.A., Mahmud, S., Islam, A., Ahmed, S., Siddiqui, A.B.F., Babu, S.M.O.F., Hossain, P., Shahriar, A., Nainu, F., Bin Emran, T., Simal-Gandara, J., 2021. A molecular modelling approach for identifying antiviral selenium-containing heterocyclic compounds that inhibit the main protease of SARS-CoV-2: an in silico investigation. Bioinform Brief. https://doi.org/10.1093/bib/bbab045.
Rayne, S., Mazza, G., 2007. Biological activities of extracts from sumac (Rhus spp.): A review. Plant Foods Hum. Nutr. 62, 165–175. https://doi.org/10.1007/s11130-007-0058-4.
Rozwarski, D.A., Grant, G.A., Barton, D.H.R., Jacobs, W.R., Sacchettini, J.C., 1998. Modification of the NADH of the isoniazid target (InhA) from Mycobacterium tuberculosis. Science (80-). 279, 98–102.
Saboo, S.S., Tapadiya, R.W.C.G.G., Khadabadi, S.S., 2014. Aphanamixis polystachya (wall.) parker - an important Ethnomedicinal plant. Int. J. Pharm. Sci. Rev. Res. 24, 25–28.
San Diego: Accelrys Software Inc., 2012. Discovery Studio Modeling Environment, Release 3.5 [WWW Document]. Accelrys Softw. Inc.
Sarkar, A., Kumar, K.A., Dutta, N.K., Chakraborty, P., Dastidar, S.G., 2003. Evaluation of in vitro and in vivo antibacterial activity of dobutamine hydrochloride. Indian J. Med. Microbiol. 21 (3), 172–178.
Schimmel, P., Tao, J., Hill, J., 1998. Aminoacyl tRNA synthetases as targets for new anti-infectives. FASEB J. 12, 1599–1609.
Senguttuvan, J., Paulsamy, S., Karthika, K., 2014. Phytochemical analysis and evaluation of leaf and root parts of the medicinal herb, Hypochaeris radicata L. for in vitro antioxidant activities. Asian Pac. J. Trop. Biomed. 4, S359–S367.
Siddhuraju, P., Becker, K., 2003. Antioxidant properties of various solvent extracts of total phenolic constituents from three different agroclimatic origins of drumstick tree (Moringa oleifera Lam.) leaves. J. Agric. Food Chem. https://doi.org/10.1021/jf020444+.
Siddhuraju, P., Manian, S., 2007. The antioxidant activity and free radical-scavenging capacity of dietary phenolic extracts from horse gram (Macrotyloma uniflorum (Lam.) Verdc.) seeds. Food Chem. 105 (3), 950–958. https://doi.org/10.1016/j.foodchem.2007.04.040.
van der Spoel, D., Lindahl, E., Hess, B., Groenhof, G., Mark, A.E., Berendsen, H.J., 2005. (CUL-ID:1560463) GROMACS: fast, flexible, and free. J. Comput. Chem. https://doi.org/10.1002/jcc.20291.
Stewart, J., Fyfe, L., Smith-Palmer, A., 1998. Antimicrobial properties of plant essential oils and essences against five important food-borne pathogens. Lett. Appl. Microbiol. 26, 118–122.
Subba, B., Basnet, P., 2014. Antimicrobial and Antioxidant Activity of Some Indigenous Plants of Nepal. J. Pharmacogn. Phytochem. 3, 62–67.
Suffredini, I.B., Sader, H.S., Gonçalves, A.G., Reis, A.O., Gales, A.C., Varella, A.D., Younes, R.N., 2004. Screening of antibacterial extracts from plants native to the Brazilian Amazon Rain Forest and Atlantic Forest. Brazilian J. Med. Biol. Res. 37 (3), 379–384. https://doi.org/10.1590/S0100-879X2004000300015.
Swargiary, A., Mahmud, S., Saleh, M.A., 2020. Screening of phytochemicals as potent inhibitor of 3-chymotrypsin and papain-like proteases of SARS-CoV2: an in silico approach to combat COVID-19. J. Biomol. Struct. Dyn. https://doi.org/10.1080/07391102.2020.1835729.
Tiwari, A.K., 2004. Antioxidants: New-generation therapeutic base for treatment of polygenic disorders. Curr. Sci. 86, 1092–1102.
Trott, O., Olson, A.J., 2010. AutoDock Vina: improving the speed and accuracy of docking with a new scoring function, efficient optimization, and multithreading. J. Comput. Chem. 31, 455–461.
Tsay, J.T., Oh, W., Larson, T.J., Jackowski, S., Rock, C.O., 1992. Isolation and characterization of the β-ketoacyl-acyl carrier protein synthase III gene (fabH) from Escherichia coli K-12. J. Biol. Chem. 267, 6807–6814. https://doi.org/10.1016/s0021-9258(19)50498-7.
Uddin, G., Rauf, A., Arfan, M., Ali, M., Qaisar, M., Saadiq, M., Atif, M., 2012. Preliminary Phytochemical Screening and Antioxidant Activity of Bergenia caliata 11, 1140–1142.
Uddin, M.Z., Paul, A., Rakib, A., Sami, S.A., Mahmud, S., Rana, M.S., Hossain, S., Tareq, A.M., Dutta, M., Emran, T.B., Simal-Gandara, J., 2021. Chemical Profiles and Pharmacological Properties with in Silico Studies on Elatostema papillosum Wedd. Molecules 26 (4), 809. https://doi.org/10.3390/molecules26040809.
Waghulde, S., Kale, M.K., Patil, V., 2019. Brine Shrimp Lethality Assay of the Aqueous and Ethanolic Extracts of the Selected Species of Medicinal Plants. Proc. 41, 47. https://doi.org/10.3390/ecsoc-23-06703.
Wang, G.-W., Jin, H.-Z., Zhang, W.-D., 2013. Constituents from Aphanamixis species and their biological activities. Phytochem. Rev. 12 (4), 915–942. https://doi.org/10.1007/s11101-013-9317-1.
Wang, J., Wolf, R.M., Caldwell, J.W., Kollman, P.A., Case, D.A., 2004. Development and testing of a general Amber force field. J. Comput. Chem. 25 (9), 1157–1174. https://doi.org/10.1002/(ISSN)1096-987X10.1002/jcc.v25:910.1002/jcc.20035.
Wang, N.-N., Huang, C., Dong, J., Yao, Z.-J., Zhu, M.-F., Deng, Z.-K., Lv, B., Lu, A.-P., Chen, A.F., Cao, D.-S., 2017. Predicting human intestinal absorption with modified random forest approach: a comprehensive evaluation of molecular representation, unbalanced data, and applicability domain issues. RSC Adv. 7 (31), 19007–19018. https://doi.org/10.1039/C6RA28442F.
XiaoPing, C., Yan, C., ShuiBing, L., YouGuo, C., JianYun, L., LanPing, L., 2009. Free radical scavenging of Ganoderma lucidum polysaccharides and its effect on

antioxidant enzymes and immunity activities in cervical carcinoma rats. Polym. Carbohydr. https://doi.org/10.1016/j.carbpol.2009.01.009.

Zaffer, M., Ahmad, S., Sharma, R., Mahajan, S., Gupta, A., Agnihotri, R.K., 2014. Antibacterial activity of bark extracts of Moringa oleifera Lam. against some selected bacteria. Pak. J. Pharm. Sci. 27, 1857–1862.

Zalewska-Piątek, B., Piątek, R., 2020. Phage therapy as a novel strategy in the treatment of urinary tract infections caused by e. Coli. Antibiotics 9, 1–20. https://doi.org/10.3390/antibiotics9060304.

Zhang, A., Sun, H., Wang, X., 2013. Recent advances in natural products from plants for treatment of liver diseases. Eur. J. Med. Chem. 63, 570–577. https://doi.org/10.1016/j.ejmech.2012.12.062.

Zhishen, J., Mengcheng, T., Jianming, W., 1999. The determination of flavonoid contents in mulberry and their scavenging effects on superoxide radicals. Food Chem. 64 (4), 555–559. https://doi.org/10.1016/S0308-8146(98)00102-2.